Biomaterials 98 (2016) 64–78

Contents lists available at ScienceDirect

Biomaterials

journal homepage: www.elsevier.com/locate/biomaterials

Myocardial commitment from human pluripotent stem cells: Rapid production of human heart grafts

Elena Garreta [a, 1], Lorena de Oñate [a, b, 1], M. Eugenia Fernández-Santos [c, d], Roger Oria [e, f], Carolina Tarantino [a], Andreu M. Climent [g], Andrés Marco [a], Mireia Samitier [a], Elena Martínez [h], Maria Valls-Margarit [h], Rafael Matesanz [i], Doris A. Taylor [j, k, l], Francisco Fernández-Avilés [c, d, ***], Juan Carlos Izpisua Belmonte [m, **], Nuria Montserrat [a, *]

[a] Pluripotent Stem Cells and Activation of Endogenous Tissue Programs for Organ Regeneration, Institute for Bioengineering of Catalonia (IBEC), Barcelona, Spain
[b] Center of Regenerative Medicine in Barcelona (CMRB), Barcelona, Spain
[c] Department of Cardiology, Hospital General Universitario Gregorio Marañón, Universidad Complutense de Madrid, Spain
[d] Cell Production Unit, Department of Cardiology, Instituto de Investigación Sanitaria Hospital Gregorio Marañón (IiSGM), Madrid, Spain
[e] Institute for Bioengineering of Catalonia (IBEC), Barcelona, Spain
[f] University of Barcelona, Barcelona, Spain
[g] Bioartifical Organs Laboratory, Instituto de Investigación Sanitaria Hospital Gregorio Marañón (IiSGM), Madrid, Spain
[h] Biomimetic Systems for Cell Engineering, Institute for Bioengineering of Catalonia (IBEC), Barcelona, Spain
[i] National Transplant Organization (ONT), Spanish Ministry of Health and Consumption, Spain
[j] Center for Cardiovascular Repair, University of Minnesota, Minneapolis, MN, USA
[k] Department of Regenerative Medicine Research, Texas Heart Institute, Houston, TX, USA
[l] Department of Integrative Biology and Physiology, University of Minnesota, Minneapolis, MN, USA
[m] Gene Expression Laboratory, Salk Institute for Biological Studies, La Jolla, CA, USA

ARTICLE INFO

Article history:
Received 16 December 2015
Received in revised form
1 April 2016
Accepted 4 April 2016
Available online 26 April 2016

Keywords:
Gene targeting
Pluripotent stem cells
Extracellular matrix
Cardiac function

ABSTRACT

Genome editing on human pluripotent stem cells (hPSCs) together with the development of protocols for organ decellularization opens the door to the generation of autologous bioartificial hearts. Here we sought to generate for the first time a fluorescent reporter human embryonic stem cell (hESC) line by means of Transcription activator-like effector nucleases (TALENs) to efficiently produce cardiomyocyte-like cells (CLCs) from hPSCs and repopulate decellularized human heart ventricles for heart engineering. In our hands, targeting myosin heavy chain locus (MYH6) with mCherry fluorescent reporter by TALEN technology in hESCs did not alter major pluripotent-related features, and allowed for the definition of a robust protocol for CLCs production also from human induced pluripotent stem cells (hiPSCs) in 14 days. hPSCs-derived CLCs (hPSCs-CLCs) were next used to recellularize acellular cardiac scaffolds. Electrophysiological responses encountered when hPSCs-CLCs were cultured on ventricular decellularized extracellular matrix (vdECM) correlated with significant increases in the levels of expression of different ion channels determinant for calcium homeostasis and heart contractile function. Overall, the approach described here allows for the rapid generation of human cardiac grafts from hPSCs, in a total of 24 days, providing a suitable platform for cardiac engineering and disease modeling in the human setting.

* Corresponding author. Pluripotent stem cells and activation of endogenous tissue program for organ regeneration. Institute for Bioengineering of Catalonia (IBEC), C/ Baldiri Reixac 15-21, 08028-Barcelona, Spain.
** Corresponding author. Gene Expression Laboratory, Salk Institute for Biological Studies, 10010 North Torrey Pines Road, La Jolla, California 92037, USA
*** Corresponding author. Department of Cardiology, Hospital General Universitario Gregorio Marañón, University Complutense of Madrid, C/ Dr Esquerdo 46, 28007 Madrid, Spain.
E-mail addresses: faviles@secardiologia.es (F. Fernández-Avilés), belmonte@salk.edu (J.C. Izpisua Belmonte), nmontserrat@ibecbarcelona.eu (N. Montserrat).
[1] Both authors equally contributed to the development of the work presented here.

http://dx.doi.org/10.1016/j.biomaterials.2016.04.003

1. Introduction

The derivation of human embryonic stem cells (hESCs) [1] together with the finding that human somatic cells could be converted towards human induced pluripotent stem cells (hiPSCs) [2] opened new venues for the production of protocols aiming to generate patient cardiac-like cells (CLCs) with an impact in heart regenerative therapies [3]. Recently, organ decellularization is envisioned as an attractive strategy for the development of biofunctional organs for drug screening and personalized medicine [4–8]. In the last years, several works have proved the feasibility to use cardiac extracellular matrix (ECM) from murine, pig or rat origin for cardiac engineering using human ESCs (hESCs) [9–11]. Interestingly, CLCs derived from human iPSCs (hiPSCs-CLCs) have recently proved to repopulate human hearts [4]. Here we describe a rapid protocol for the generation of human cardiac grafts by co-culturing hESCs and hiPSCs (human pluripotent stem cells-hPSCs) on cardiac ECM from human origin avoiding the use of extensive culture in bioreactors. Moreover, our experimental setting allowed for the investigation of the effect of human ventricular decellularized ECM (vdEMC) on electrophysiological responses related to cardiac function.

Protocols for derivation of cardiac like cells (CLCs) from hPSCs (hPSCs-CLCs) have traditionally relied on the time consuming production of embryoid bodies (EBs), achieving low yields of CLCs generation, thus hampering the reproducibility and scale up of such procedures [3,12,13]. Interestingly, in the last years several authors, including us, have demonstrated that is possible to induce cardiac differentiation from hPSCs grown as monolayers [14–17]. Although challenging, those protocols still did not provide exact information about the identity of the generated cells. In this regard, the generation of cardiac hPSCs reporter cell lines may lead to the definition of the developmental cues driving cardiac differentiation, and more importantly, to develop rapid methods for the enrichment of different cardiac cell types during the onset of differentiation. So far only two previous reports using Bacterial Artificial Chromosome (BACs) showed the possibility to target cardiac-related loci in hPSCs by homologous recombination [18,19]. In the same manner, transposon-based approaches have led to the generation of hESCs reporter cell lines for cardiac differentiation [20,21]. These studies showed that reporter hPSCs lines could lead to the identification of novel markers for hPSCs-CLCs generation and expansion *in vitro*. In the last years, genome editing technologies as CRISPR/Cas9 and TALEN platforms, have emerged as powerful tools for targeting in site-specific manner unique and multiple human loci, allowing to study gene function, disease modeling and drug discovery, among other applications. To our knowledge, neither CRISPR/Cas9 nor TALEN platforms have been explored for the generation of cardiac reporter hPSCs lines.

MYH6 is an important transcription factor essential for cardiac muscle contraction, and recently, mouse MYH6-GFP fibroblasts have been used for the study of cardiac conversion [22]. Based on those findings, and taking advantage of TALEN technology, we have targeted human MYH6 locus with mCherry fluorescent reporter preserving the regulatory sequences near the native ATG start codon for translation of MYH6 gene. In our hands, TALEN engineering and subsequent cell culture pressure did not hamper mCherry MYH6 reporter hESC line to exhibit classical pluripotent-related features, and more importantly, enabled us to define a robust protocol for the generation of CLCs from different hPSC lines. Next, we made use of our recently reported method of perfusion decellularization in human hearts for the generation of vdECMs constructs. After only 10 days, hPSCs-CLCs grown on human vdECMs exhibit a higher degree of physiological and molecular cardiac differentiation compared to hPSCs-CLCs counterparts cultured in matrigel substrates. Overall, here we set up a rapid protocol for the development of human heart grafts for drug screening and disease modeling applications.

2. Methods

2.1. Donor heart harvest and heart decellularization

Between May 2010 and June 2013, we harvested 52 human hearts that were determined by the Spanish National Transplant Organization (ONT) as not suitable for transplantation. The ONT is part of the Spanish Ministry of Health and Consumption and is in charge of coordinating the donation, extraction, preservation, distribution, exchange, and transplantation of organs, tissues, and cells throughout the Spanish Health Care System. Approval for all studies was obtained from the relevant investigation and ethics committees of the Hospital General Universitario Gregorio Marañón on and from the ONT. The relatives of each donor provided an informational brochure stating that the heart would be used for this investigational purpose. After approval was obtained, and other organs suitable for transplantation were explanted, we used standard transplantation protocols to remove the heart. Briefly, a median sternotomy was performed to expose the mediastinum, the pericardium was opened, and the superior and inferior vena cava were dissected. The hearts were maintained in saline at 4 °C until decellularization was performed within few hours after harvesting.

We used our previously described perfusion decellularization protocol to remove the cells from the heart while retaining the ECM [5]. Briefly, hearts were perfused with 1% sodium dodecyl sulfate (SDS) in deionized water via antegrade flow through the ascending aorta; perfusion was stopped at day 4–8. Hearts were then rinsed extensively with approximately 20 L of phosphate-buffered saline (PBS). Thirteen hearts were not decellularized and served as cadaveric controls. Thick slices (400 μm) of decellularized heart ventricles were obtained using a vibratome, and further seeded with hPSCs-CLCs. Slices were kept at 4 °C in PBS in the presence of penicillin and streptomycin (Penicillin 10.000 U/ml:Streptomycin 10.000 μg/ml-Invitrogen#15140-122) until further use.

2.2. DNA quantification

To assess total DNA content in the ECM scaffolds, samples were digested as described previously [23]. After isolation, DNA content was quantified using the Picogreen DNA assay following manufacturer's instructions (Invitrogen).

2.3. Cell lines

Control fibroblasts (ATCC® SCRC-1041) were grown in DMEM supplemented with 10% fetal bovine serum, 2 mM L-glutamine, 0.1 mM 2-mercaptoethanol, nonessential amino acids and penicillin-streptomycin (Penicillin 10.000 U/ml:Streptomycin 10.000 μg/ml-Invitrogen#15140-122). hESC ES4 line from Banco Nacional de Lineas Celulares and hiPSCs (FiPS#1 line) were grown in mTeSR1 (05850, Stem Cell Technologies) in matrigel substrate (354277, Corning) following manufacturer recommendations.

2.4. Antibodies

The following antibodies were used: tumor rejection antigen 1 (TRA-1), TRA-1–81 (MAB4381, 1:100, Chemicon); OCT-3/4 (sc-5279, 1:25, Santa Cruz Biotechnology); NANOG (AF1997, 1:25, R&D Systems); Paired Box 6 (PAX6, PRB-278P, 1:100, Covance); Microtubule-Associated Protein 2 (MAP2, sc-32791, 1:25, Santa

Cruz Biotechnology) α1-fetoprotein (AFP, A0008, 1:200, Dako); Forkhead Box Protein A2 (FOXA-2, AF2400, 1:50, R&D Systems); α-sarcomeric actinin (ASA, A7811, 1:100, Sigma); RFP (ab34771, 1:400, Abcam); Myosin Heavy Chain (MYH6, GTX20015, 1:100, GeneTex); GATA 4 binding 4 (GATA4, sc9053, 1:25, Santa Cruz Biotechnology); NKX2.5 (sc8697, 1:25, Santa Cruz Biotechnology); Troponnin T (TNN, MS-295-P1ABX, 1:500, Thermo Scientific); Collagen Type IV (CIV22; ref: 760-2632; Dako); Actin Muscle Specific (HHF 35; ref: 760-260; Roche); Desmin (DE-R-11; ref 760-2513; Roche). Secondary antibodies used were all the Alexa Fluor Series from Jackson Immunoresearch (all 1:200). For immunohistochemistry anti-Mouse HRP-DAB Cell & Tissue Staining Kit (R&D, CTS002). Images were taken using a Leica SP5 confocal microscope and Nikon-TE200.

2.5. Genome editing of human embryonic stem cells with TALENs

TALENs were designed and assembled as described [24,25]. Each TALEN consists of 34 amino acids, where the TALEN repeat variable diresidues (RVDs) in the 12th and 13th amino acid positions of each repeat specify the DNA base being targeted according to the code: NG = T, HD = C, NI = A, and NN = G or A. Tandem arrays of customized TALE repeats were assembled using hierarchical ligation and combining separate digest and ligation steps into single Golden Gate reactions [26,27]. First, each nucleotide-specific monomer sequence: NI, HD, NG, NN (from TALE Toolbox kit Addgene cat no: 100000019) was amplified with ligation adaptors that uniquely specify the monomer position within the future TALE tandem repeats, thus generating a monomer library. Once TALEN targeting sites were identified using TAL effector Nucleotide Targeter program [28], for each 20 bp TALEN target desired (5′ and 3′), the appropriate monomers were ligated into hexamers and amplified via PCR (specific primers were provided in TALE toolbox kit Addgene cat no: 100000019- Table S1). Then, by a second Golden Gate digestion-ligation with the appropriate TALE cloning back- bone (pCMV_NLS (NI,HD, NG, NN)_FokI), the desired MYH6 sequence-specific TALEN were fully assembled. TALEN Backbone was a gift from Feng Zhang (Addgene plasmid # 31179) [24]. All TALENs used the +63 truncation point [25]. The complete sequence of all TALENs used in this work is provided in supplementary information (Fig. S1). After Sanger analysis for verification, HEK 293 cells were transfected with TALENs as described previously [25,29]. Four hundred thousand cells were transfected, and subsequently genomic DNA was extracted without selecting for transfected cells using DNeasy Blood & Tissue kit (Qiagen). TALEN activity was assayed via Surveyor nuclease assay (Transgenomic) using the following primers for the amplification of the expected targeting area: Surveyor MYH6 Forward 5'- cactcagcgccaacccttagcatactccag-3′ and Surveyor MYH6 Reverse 5'-ccaggggtgattctcttggctggtgtgag-3'. Primers were used at a final concentration of 1 μM each in 50 μL reactions using TAKARA LA Taq pol Hot Start (Takara). PCR reactions were as follows: an initial denaturation step (94 °C, 1 min); next, 35 cycles of a denaturation step of 20 s at 94 °C, annealing and extension step of 5 min at 68 °C, and a final extension step of 10 min at 72 °C. After absolute quantification of PCR products, 800 ng were used to perform the DNA heteroduplex formation on a 96 well thermocycler with programmable temperature stepping functionality (Applied Biosystems) and following transgenomic Surveyor mutation detection kit (Life Technologies) indications.

2.6. MYH6 donor vector (d-vector) design and construction

MYH6 donor vector (MYH6 d-vector) was generated by In-Fusion® cloning method (Clonetech) following manufacturer's indications. MYH6 genomic sequence was purchased in BACPAC Resources Center (RP11-929J10; BPRC) and used as template for 1 Kb homology arms amplification by PCR. Then, HA_mCherry_Poly cassette was amplified from pCAG_HA_mCherry_Poly based vector from The Scripps Institute [30] by adding an extra Kozac sequence to enhance mCherry future expression. A first In-Fusion® reaction was done with 25 ng of pZero_FRT_Neo [31] double digested with *BamHI* and *NdeI* restriction enzymes (New England Biolabs) and pZero_5'arm_HAmCherry_FRT_Neo was generated. Next MYH6 3′ homology arm was cloned by a second In-Fusion® reaction on pZero_5'arm_HAmCherry_FRT_Neo vector digested with *EcoRV* and *XhoI* restriction enzymes (New England Biolabs) to generate a final donor vector: pZero_5'arm_HAmCherry_FRT_Neo_3'arm (Fig. S2). PCRs were performed with primers listed on Table S2. PCR conditions were: 3 min at 94 °C; 30 cycles of denaturation at 94 °C for 30 s, primer annealing at 60 °C for 30 s, extension at 68 °C for 1–2 min and final extension step of 5 min at 65 °C.

2.7. Targeting of hESCs using TALEN mediated homologous recombination

ES4 was cultured in 10 μM Rho Kinase (ROCK)-inhibitor (Calbiochem; Y-27632) 1–3 h prior to electroporation. Cells were harvested using Accumax (Stem Cell Technologies cat no 07921) and 1×10^6 cells resuspended in 800 μL phosphate buffered saline (PBS) and 15 μg of each pair of TALEN constructs (30 μg total) plus 30 μg of donor vector were added into cell suspensions. Electroporation conditions were fixed at 500 μF; 200Ω; 250 V in Gene Pulser Xcell™. 72 h after electroporation cells were selected by the acquisition of Neomycin resistance adding 50 μg/ml of Neomycin (G418, GIBCO). Targeted clones were selected by two different PCR reactions with GXL polymerase (TAKARA). Primers for short and long PCR products are listed in Table S3.

2.8. Southern blot analysis on targeted ES4 clones

Genomic DNA from ES4 clones positive for targeting by PCR screening was isolated using All Prep DNA/RNA columns (Qiagen) following manufacturer's guidelines. Briefly, 5 μg of genomic DNA was digested with 40 U of *BclII* restriction enzyme (New England Biolabs) overnight and separated by electrophoresis on a 1% agarose gel. Next, DNA was transferred to a neutral nylon membrane (Hybond-N, Amersham) and hybridized with DIG-dUTP labeled probes generated by PCR using the PCR DIG Probe Synthesis Kit (Roche Diagnostics). Probes were detected by an AP-conjugated DIG-Antibody (Roche Diagnostics) using CDP-Star (Sigma-Aldrich) as a substrate for chemiluminescence. Primers for probe synthesis are listed in Table S4. Genomic DNA from clone #3 was verified by Sanger (Fig. S3).

2.9. Reprogramming of human fibroblasts

Episomal plasmids published elsewhere [32] were used to generate hiPSCs lines in a period of only 20–22 days. Fibroblasts were cultured and maintained in fibroblasts media: DMEM (Invitrogen, cat.no. 11965-092), 10% FBS (Invitrogen, cat. no. 10270-106), 1 mM Glutamax (Gibco®, Life Technologies cat no.35050-038) and 50 U/ml, 50 μg/ml of Penicillin/Streptomycin (Gibco®, Life Technologies cat no.15140-122) in a humidified 37 °C 5% CO2 incubator. When cells reached 80% of confluence, 500.000 of cells trypsinized with 0.25% Trypsin/EDTA (Invitrogen, cat. no. 25200-056) and washed with PBS. Next, cells were resuspended in pre-warmed Human MSC Nucleofector Solution at room temperature. Nucleofector Solution was prepared following Human MSC Nucleofector® Kit recommendations (VPE-1001, Amaxa). Then, plasmid mixture containing 1 μg of each pCLXE episomal based plasmid were added

to the nucleofection solution [pCXLE-hSK (Addgene plasmid # 27078), pCXLE-hOCT3/4-shp53-F (Addgene plasmid #27077), pCXLE-hUL (Addgene plasmid #27080) were a gift from Shinya Yamanaka]. Nucleofection reaction was performed in a provided Amaxa certified cuvette using nucleofection program U-23 from the Nucleofector™ 2b Device (Amaxa cat.no. AAB-1001). Cells were immediately transferred into two wells of a six-well culture plate with pre-warmed fibroblast culture media and incubated for 4 additional days with daily media change. Finally, nucleofected cells were subcultured onto matrigel (354277, Corning) coated plates in the presence of mTeSR1 (05850, Stem Cell Technologies).

2.10. Induced pluripotent stem cells generation and subculture

On day 23 hiPSC colonies were picked manually and expanded in matrigel (354277, Corning) coated plates in the presence of mTeSR1 (05850, Stem Cell Technologies). From this stage on hiPSC colonies were amplified by trypsinization in matrigel (354277, Corning).

2.11. Immunocytochemistry and fluorescence microscopy

ES4 and ES4 TALEN mCherry_MHY6/wt #3 (ES4 mCherry_MYH6), FiPS#1 line, hPSCs-CLCs, ventricular decellularized ECMs (vdECMs) and recellularized vdECMs were fixed in 2% paraformaldehyde in PBS. After fixation, samples were blocked and permeabilized for 1 h at room temperature in the presence of 0.5% Triton X100 and 6% donkey serum. Subsequently, samples were incubated with the indicated primary antibodies overnight at 4 °C. Samples were then washed thrice with PBS and incubated for 2 h at room temperature with the respective secondary antibodies. Samples were washed thrice with PBS and counterstained with DAPI (Invitrogen) before analysis. Samples were imaged using a SP5 (Leica) microscope.

2.12. RT-PCR analysis

Total RNA was isolated using All Prep RNA columns (Qiagen) according to the manufacturer's recommendations. 2 μg of TURBO™ DNase (Ambion, AM2238) treated total RNA was used for cDNA synthesis using the SuperScript II Reverse Transcriptase kit for RT-PCR (Invitrogen). Real-time PCR was performed using the SYBR Green PCR Master Mix (Applied Biosystems) in an ABI Prism 7300 thermocycler (Applied Biosystems) and primers (Table S5).

2.13. In vitro differentiation of human pluripotent stem cell lines

ES4 mCherry_MYH6 line was differentiated *in vitro* towards the three germ layers of the embryo. Monolayers of hPSCs were disaggregated and subsequently induced to form Embryoid Bodies (EBs) by centrifugation of cells within round-bottomed low attachment 96-well plates at 950 g for 5 min as described elsewhere [33]. After 3–4 days EBs were transferred to 0.1% gelatin-coated glass chamber slides and cultured in differentiation medium (DMEM supplemented with 20% fetal bovine serum, 2 mM L-glutamine, 0.1 mM 2-mercaptoethanol, nonessential amino acids and penicillin-streptomycin) for 2–3 weeks to allow spontaneous endoderm formation. The medium was changed every other day. For mesoderm differentiation, EBs were maintained on gelatin-coated glass chamber slides in differentiation medium supplemented with 100 μM ascorbic acid (Sigma). For ectoderm differentiation, EBs were cultured on matrigel coated glass chamber slides in N2B27 medium (DMEM/F12 and neurobasal medium 1:1 supplemented with 1% N2 (Invitrogen), 0.5% B27 (Invitrogen), 2 mM L-glutamine and penicillin-streptomycin) supplemented with 1 μM retinoic acid (Sigma) for 2–3 weeks. The medium was changed every other day.

2.14. In vitro generation of cardiomyocyte-like cells (CLCs) from human pluripotent stem cells (hPSCs)

Single cell suspension of hPSCs were seeded onto matrigel (BD Biosciences) pre-coated cell culture dishes at a density of 125,000 cells per cm^2 in mTeSR medium (StemCell Technologies). Cells were then maintained in mTeSR for 48 h. Differentiation was initiated by treatment with 12 μM CHIR99021 (Selleck) in RPMI (Invitrogen) supplemented with B27 minus insulin (Life Technologies), 2 mM L-glutamine, 0.1 mM 2-mercaptoethanol, nonessential amino acids and penicillin-streptomycin (RPMI/B27-insulin medium) for 24 h (day 0 to day 1). On day 1, inhibitor was then removed by intensive washing once with RPMI and medium was changed to RPMI/B27-insulin. On day 3, cells were treated with 5 μM Wnt inhibitor IWP4 (Stemgent) in RPMI/B27-insulin medium and cultured without medium change for 48 h. On day 5, cells were washed once with RPMI to eliminate the inhibitor and maintained in RPMI (Invitrogen) supplemented with B27 (Life Technologies), 2 mM L-glutamine, 0.1 mM 2-mercaptoethanol, nonessential amino acids and penicillin-streptomycin (RPMI/B27 medium). From day 5, cells were maintained in RPMI/B27 medium with medium change every 2 days. On day 14, beating monolayers were obtained.

2.15. Flow cytometry

Cells were disaggregated from cell culture plates by incubation with Accumax (Invitrogen) for 5 min at 37 °C. Cells were vortexed to disrupt the aggregates, and neutralized by adding DMEM medium containing 10% fetal bovine serum (FBS). Next cells were washed once in PBS without Ca/Mg^{2+} supplemented with 0.1 mM EDTA (fluorescence-activated cell sorter (FACS) buffer), and resuspended in 500 μL of FACS buffer for analysis. Approximately one million cells were used for each flow sample. Data were collected and analyzed on an Aria FUSION (Becton Dickinson) flow cytometer.

2.16. Second harmonic generation (SHG) and two-photon excited fluorescence (TPEF)

Heart ECM was imaged by a nonlinear technique of SHG and TPEF. This technique enables noninvasive visualization of collagen and elastin in intact unstained tissues [34–36]. Collagen is a non-centrosymmetric molecule that efficiently generates the second harmonic of incident light, while elastin is a significant source of ECM autofluorescence that can be imaged by TPEF. The SHG-TPEF setup consisted of a Leica inverted confocal laser scanning microscope SP-5 with META scanning module equipped with a mode-locked near-infrared MAITAI Wide Band (710 nm-990 nm) laser (Spectra Physics Millennia Pro 10sJ). The exciting laser beam was tuned to 900 nm and the SHG collagen signal was obtained using a 447–453 nm bandpass filter. The TPEF signal was collected in a second channel by tuning the exiting laser beam to 810 nm, using a 460–600 nm bandpass filter. DAPI stained nuclei in hPSCs-CLCs grown on vdECMs were detected in the same channel as elastin. Images were taken using a Leica HCX PL APO CS 40.0 × 1.25-NA oil-immersion objective.

2.17. Strain analysis

Measurements of contractile strain were performed by recording high resolution microscopical movies by using a (EMCCD; Evolve-128: 128 × 128, 24 × 24 μm-square pixels, 16 bit;

Photometrics, Tucson, AZ, USA) mounted in an OLYMPUS Stereo Microscope MVX10 (0.63 × objective). Specifically, 500 frames per second were acquired with a spatial resolution of 39 μm per pixel. Total area covered by the image was 5 × 5 mm. Custom software written in MATLAB was used to measure the deformation of culture due to cardiac cells contraction. Maximal strain capacity was measured as the ratio of elongation in the direction of maximal contraction.

2.18. Optical mapping

Simultaneous voltage and calcium imaging was developed by recording emission light of di-4-ANBDQPQ (provided by Dr Leslie M. Loew from the Richard D. Berlin Center for Cell Analysis and Modeling, University of Connecticut Health Center, USA) and rhod-2(AM) (Ca2+ sensitive probe, TEFLabs, Inc, Austin, TX. USA) respectively. The optical mapping system (Essel Research, Toronto, Canada) consisted in a multiple light-emitting diodes as excitation light sources and a high-speed an electron- multiplying charge-coupled device (EMCCD) camera as recording system [37]. Specifically, in order excite voltage dye di-4-ANBDQPQ, cell cultures were illuminated with a filtered red LED light source: LED CBT-90-B (peak power output 53 W; peak wavelength 460 nm; Luminus Devices, Billerica, MA, USA) with a plano-convex lens (LA1951; focal length 0 25.4 mm; Thorlabs, New Jersey, USA) and a red excitation filter (D470/20X (Chroma Technology, Bellows Falls, VT, USA). In order to excite calcium dye rhod-2, cell cultures were illuminated with a filtered green LED light source: LED: CBT-90-G (peak power output 58 W; peak wavelength 524 nm; Luminus Devices, Billerica, USA), with a plano-convex lens (LA1951; focal length = 25.4 mm; Thorlabs, New Jersey, USA) and a green excitation filter (D540/25X; Chroma Technology, Bellows Falls, USA). Two such light sources were used to achieve homogeneous illumination. Fluorescence was recorded with EMCCD camera (Evolve-128: 128 × 128, 24 × 24 μm-square pixels, 16 bit; Photometrics, Tucson, AZ, USA), with a custom multiband-emission filter (ET585/50-800/200 M; Chroma Technology) placed in front of a high-speed camera lens (DO-2595; Navitar Inc., Rochester, USA). Custom software written in MATLAB was used to control the system and to perform optical mapping image processing.

2.19. Optical mapping dye loading

For calcium transient (CaT) imaging, hPSCs-CLCs were stained by immersion in 3 mL of a modified Krebs solution at 36.5 °C (containing, in mM: NaCl, 120; NaHCO3 25; CaCl2 1.8; KCl 5.4; $MgCl_2$ 1; glucose 5.5; H2O4PNa·H2O 1.2) with rhod-2 AM dissolved in DMSO (1 mM stock solution; 3.3 μl per ml in culture medium) and Probenecid (TEFLabs, Inc, Austin, TX, USA) at 420 μM for 30 min under incubation conditions. After calcium dye incubation, culture medium was changed to fresh modified Krebs with di-4-ANBDQPQ voltage dye [38] dissolved in pure ethanol (27.3 mM stock solution, 2 μl per ml in culture medium) and Pluronic F-127 (Life Technologies) was added to a final concentration of 0.2–0.5%]. After voltage dye incubation during 5 min, culture medium was changed to fresh Krebs solution at 36.5 °C supplemented with 10 μM blebbistatin. All chemicals were obtained from Sigma-Aldrich (Dorset, UK) or Fisher Scientific Inc. (New Jersey, USA).

2.20. Spinning disk confocal microscopy

Images of beating hPSCs-CLCs monolayers and co-cultures on vdECMs were acquired using a CFI Plan Achromat UW 2× objective in a spinning disk confocal microscope (Andor). hPSCs-CLCs cultures were maintained at 37 °C in RPMI/B27 medium and imaged every 50 and 100 m for 20–30 s. Images were exported into ImageJ for processing.

2.21. Statistical analysis

Data are mean ± SD. mRNA expression by qPCR during the time course of cardiac differentiation was analyzed with one-way ANOVA and Bonferroni post-test. Different letters indicate significant difference between groups ($p < 0.05$). When analyzing statistical differences between two different experimental groups (matrigel and vdECMs culture systems) two-tailed student's *t*-test was used. Results were considered statistically significant if the p-value was less than *0.05, **0.01 and ***0.001. Statistical analysis were performed using Graph Pad 5.0 and SPSS (v.11).

3. Results

3.1. TALEN-mediated targeting of the MYH6 locus in human embryonic stem cells (hESCs) does not affect pluripotency-associated features

We made use of TALEN technology to target the MYH6 human locus in hESC, namely ES4 line (Fig. S4). Following design and assembly of the *in silico* designed TALEN pairs (Table S1) TALEN endonuclease-associated activity was tested in HEK293 cells prior to genome engineering of ES4 line by means of Surveyor nuclease assay (Fig. S5). We then evaluated the efficiency of the best TALEN pair for producing a knock in reporter allele by targeting the MYH6 human locus using drug selection. The DSB induced in ES4 line was subsequently repaired through homologous recombination (HR) with MYH6 donor vector (Fig. 1A). Thus after clone expansion and antibiotic selection we identified 24 putative mCherry_MYH6 targeted ES4 clones resistant for Neomycin that were subsequently analyzed by PCR screening, identifying a total of 18 out of 24 positively targeted ES4 clones when TALEN pair 1 was used (Fig. S6). Southern blot analysis was performed in 4 out of 18 putative MYH6 targeted clones, revealing that 3 of them contained a MYH6 targeted allele (Fig. S7).

We proceed to characterize one of those clones, namely ES4 TALEN mCherry_MHY6/wt #3 (ES4 mCherry_MYH6), for the expression of nuclear transcription factors as OCT4, NANOG and TRA-1-81 surface marker by immunofluorescence, confirming their pluripotent nature (Fig. 1B). We next explored if gene targeting hampered ES4 mCherry_MYH6 differentiation towards the three germ layers of the embryo and we found that ES4 mCherry_MYH6 line exhibited the capacity to generate cells from ectodermal, mesodermal and endodermal lineages (Fig. 1C). Remarkably, mCherry expression was limited to the cardiac mesodermal lineage and not found in the ectoderm and endoderm germ layers, indicating a proper response of our reporter cell line under differentiation (Fig. 1C). In addition, ES4 mCherry_MYH6 line exhibited the classical ES-associated morphology (Fig. 1D, top panel), and continued to express pluripotent-related markers, including Dppa4, Nanog, Oct4, Rex1, Sox2, Cripto, Dnmt3b, Sall2 and Utf1 (Fig. 1D, bottom panel).

3.2. Chemically defined media sustains cardiac differentiation from hPSCs

To demonstrate that ES4 mCherry_MYH6 line recapitulated MYH6 activity, we established a protocol for the generation of cardiac-like cells (CLCs) from hPSCs (hPSCs-CLCs) grown as monolayers based on a stage specific activation and suppression of the canonical Wnt signaling. Concisely, ES4 mCherry_MYH6 cells were exposed to GSK3B inhibitor (CHIR99021) from day 0 to day 1,

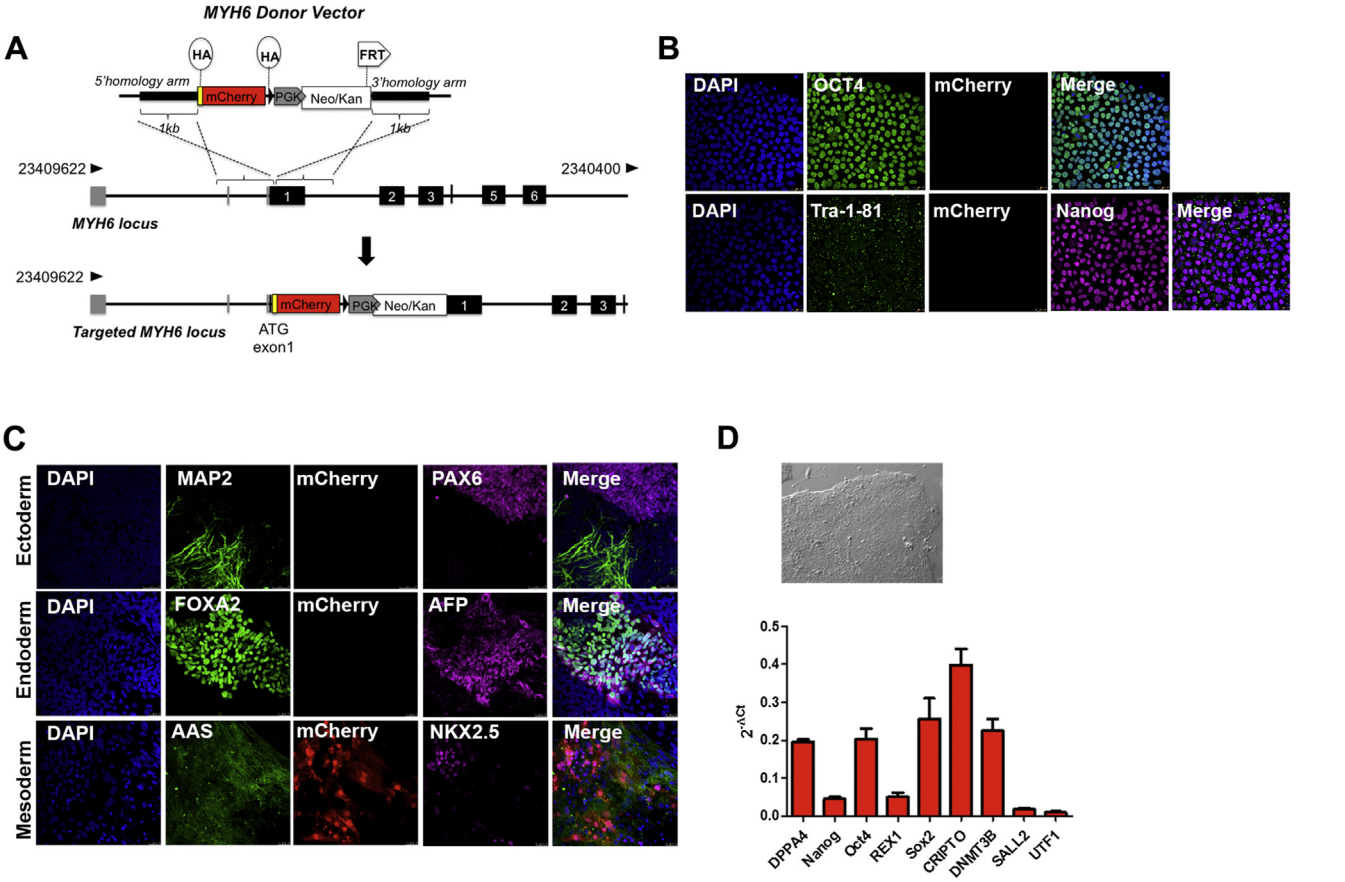

Fig. 1. TALEN engineering in hESCs. A. MYH6 donor vector includes a mCherry cassette HA-tagged (HA), a PGK promoter and a neomycin-kanamycin resistant cassette (Neo/Kan); both flanked by FRT sites. Dashed lines indicate the sites of HR in the *MYH6* locus. HR results in *knock in* of the complete cassette into the ATG start site of *MYH6* locus, generating a mCherry-tagged *MYH6* allele. **B** Immunodetection for OCT4, NANOG and TRA-1–81 in ES4 mCherry_MYH6 line, (scale bars, 50 μm). Note mCherry signal was not detected. **C** *In vitro* differentiation of ES4 MYH6_mCherry line into ectoderm [Microtubule-Associated Protein 2 (MAP2) and Paired Box 6 (PAX 6)], endoderm [α-fetoprotein (AFP), Forkhead box protein A2 (FOXA2)], mesoderm [K2 Homeobox 5 (NKX2.5) and α-sarcomeric actinin (ASA)], (scale bars, 25 μm). **D** *Top panel*, representative contrast phase image of an undifferentiated ES4 mCherry_MYH6 clone that grows as a compact and tight adherent colony. *Bottom panel*, qPCR analysis for the evaluation of mRNA expression of pluripotency associated markers after TALEN engineering in ES4 line. Data were represented as mean ± standard deviation.

followed by Wnt production-4 inhibitor (IWP4) from day 3 to day 5 of differentiation. From day 5, monolayers were kept in RPMI/B27 medium (Fig. 2A). We further explored the expression of mCherry fluorescent reporter during the time course of differentiation and observed that already at day 7 mCherry fluorescent protein was detected by optical microscopy (Fig. 2B left panel). In the same manner mRNA expression analysis by qPCR showed that mCherry mRNA expression mirrored endogenous MYH6 activity, indicating the potential use of our cellular system to properly dissect cardiac differentiation from hPSCs (Fig. 2B right panel). Moreover, flow cytometric analysis showed that mCherry protein expression was present as soon as day 5 during differentiation, and that 14 days after differentiation 90% of the cells expressed mCherry fluorescent protein (Fig. 2C).

We further assessed the profile of mRNA expression during the onset of cardiac differentiation in ES4 mCherry_MYH6 line, and found out that our protocol induced the expression of mRNAs related with early mesoderm and cardiac progenitors up to day 5 during differentiation (PDGFRa, ISL-1, c-KIT). The expression of mRNAs related to cardiac program from day 5 to later stages during differentiation (GATA4, NKX2.5, MYH6, MYL2, NPPA, TNNT2, MYL7) was also analyzed. As expected, the levels of expression for pluripotent-related mRNAs as OCT4, NANOG and SOX2 markedly decreased from day 5 during differentiation (Fig. 3A and Fig. S8). Full beating monolayers were obtained at day 14 of differentiation (Video S1 and S2). Beating monolayers of ES4 mCherry_MYH6 derived CLCs (mCherry-CLCs) were also characterized by immunofluorescence for the expression of protein markers at day 14 of differentiation, showing that mCherry-CLCs expressed major proteins associated with cardiac structural function: Alpha Sarcomeric Actinin (ASA), Troponin T (TNN), Myosin Heavy Chain (MYH6); and nuclear transcription factors related to cardiac fate [K2 Homeobox 5 (NKX2.5)], together with Connexin 43 (CX43), a protein related to electrical coupling (Fig. 3B, C). In order to investigate the robustness of our protocol we further test our optimized culture conditions in both hESCs (ES4) and transgene-free and feeder-free hiPSCs derived from dermal fibroblasts (FiPS#1). Full beating monolayers were obtained from both ES4 and FiPS#1 lines after 14 days of differentiation (Video S3 and Video S4). In addition, both ES4 (Fig. S9) and FiPS#1 (Fig. S10) expressed cardiac related markers at the different selected time points as shown by qPCR. Similarly, both ES4 and FiPS#1 expressed major proteins associated with cardiac structural function after 14 days of differentiation, confirming that our culture conditions supported the generation of CLCs from different hPSC lines (Fig. S11 and Fig. S12, respectively). Altogether, our protocol sustained the derivation of hPSCs-CLCs monolayers in the presence of chemically defined media, providing a reproducible and efficient method for the generation of hPSCs-CLCs on matrigel coated plates.

Supplementary video related to this article can be found at

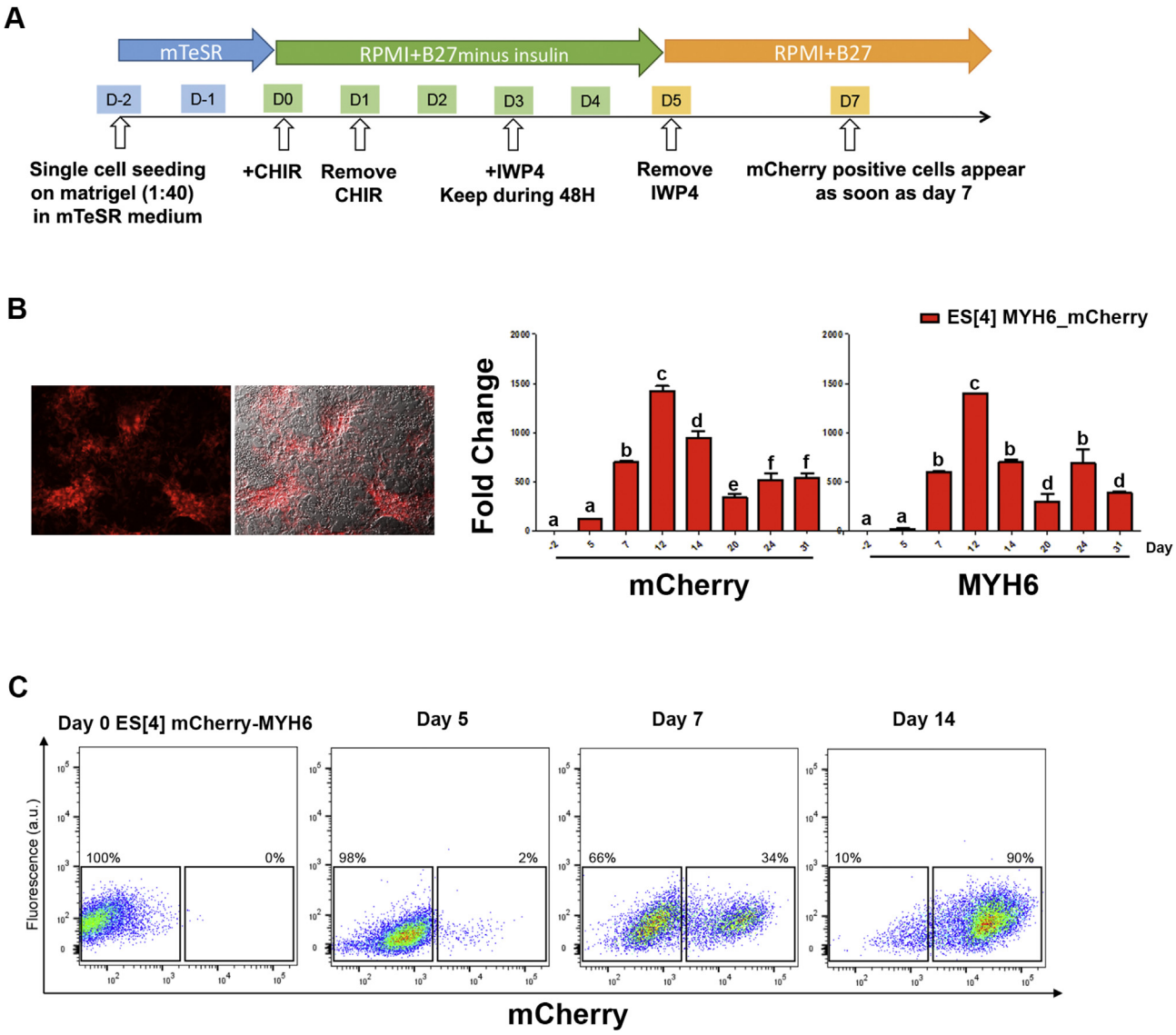

Fig. 2. mCherry targeting in MYH6 locus in ES4 line mirrors MYH6 activity during cardiac differentiation. A Time line of human ES4 mCherry_MYH6 cardiac differentiation. **B** *Left panel*, optical microscopy for mCherry detection in ES4 mCherry_MHY6 after 7 days of cardiac differentiation. *Right panel*, evaluation of mRNA expression of mCherry reporter and MHY6 gene by qPCR in ES4 mCherry_MYH6 line during the time course of cardiac differentiation at the indicated days. Data were represented as mean ± standard deviation. Different letters indicate significant differences between groups ($p < 0.05$) **C** FACS analysis for mCherry fluorescent protein during the time course of cardiac differentiation in ES4 mCherry_MYH6 at the indicated days.

http://dx.doi.org/10.1016/j.biomaterials.2016.04.003.

3.3. *In vitro recellularization of human ventricular decellularized matrices (vdECMs) with hPSCs-CLCs*

Next, we applied our previously published protocol of perfusion decellularization to generate human vdECMs scaffolds that preserved three dimensional architecture and vascular integrity [5]. Following this protocol, we prepared 400 μm thick vdECMs slices to seed hPSCs-CLCs at day 14 of differentiation in order to explore the effect of human cardiac vdECM on hPSCs-CLCs functional activity and differentiation. Prior to recellularization, immunohistochemistry against proteins from the cellular compartment including muscle specific actin and desmin, as well as basement membrane proteins of the ECM, such as collagen IV, revealed the absence of cellular content and retention of collagen IV in decellularized heart tissue scaffolds (Fig. S13A). In addition, residual DNA content in vdECMs was less than 3% (Fig. S13B), confirming a major removal of nuclear material. Furthermore, immunofluorescence analysis for laminin, collagen IV and elastin confirmed the preservation of these ECM components in our vdECMs, similarly to those in the native heart (Fig. 4A). Indeed, the presence of a dense fibrillary collagen microstructure was observed on vdECMs by SHG-TPEF microscopy (Fig. 4B). DAPI staining was not visible in vdECMs, indicating again the loss of cellular material (Fig. 4A, B). Overall, our results suggested that our decellularization protocol sufficed for the production of cardiac scaffolds that accomplished the established criteria of decellularization [39].

Next, we set up a protocol for the generation of small heart constructs for cardiac engineering by culturing mCherry-CLCs on vdECMs under our chemically defined conditions for 10 additional days. Thick slices of vdECM supported the engraftment of mCherry-CLCs, which could adhere and cover the scaffold. In this manner, spontaneously beating slices were produced and maintained in culture for 10 days (Fig. 5A). mCherry-CLCs continued to express major proteins associated with cardiac structural function [Alpha

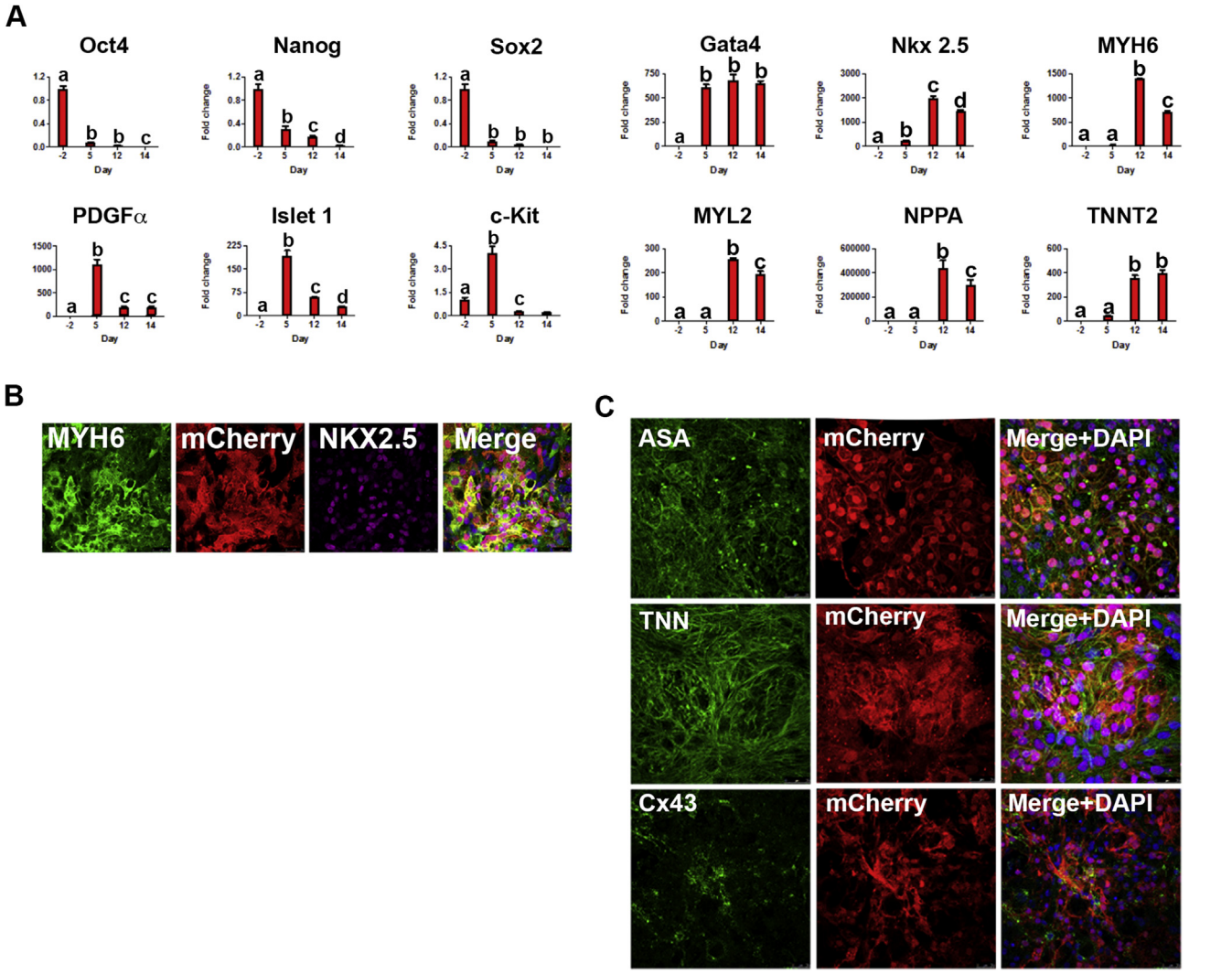

Fig. 3. Generation of CLCs from ES4 mCherry_MYH6 line. A mRNA analysis by qPCR analysis for different genes related to cardiac program and pluripotency network at the indicated days (n = 3). Data were represented as mean ± standard deviation. Different letters indicate significant differences between groups ($p < 0.05$). **B** Immunofluorescence analysis for MYH6, NKX2.5, and mCherry in mCherry-CLCs at 14 days of differentiation (scale bars, 25 μm). **C** Immunofluorescence analysis for ASA, Troponin T (TNN), Connexin 43 (CX43) and mCherry in mCherry-CLCs at 14 days of differentiation (scale bars, 25 μm).

Sarcomeric Actinin (ASA), Troponin T (TNN), Myosin Heavy Chain (MYH6)], nuclear transcription factors related to cardiac fate [K2 Homeobox 5 (NKX2.5)] and CX43 (Fig. 5B), indicating the maintenance of the cardiac phenotype after 10 days of culture with vdECMs. Interestingly, the generated cardiac grafts showed uniform contraction (Video S5 and Video S6), indicating the presence of cell-cell interconnections as well as cellular interactions with the vdECM. We subsequently transferred the same culture conditions to fabricate cardiac grafts from both ES4 derived CLCs (ES4-CLCs) and FiPS#1 derived CLCs (FiPS#1-CLCs). Cardiac grafts generated from both ES4-CLCs and FiPS#1-CLCs showed similar characteristics in terms of cardiac proteins expression (Fig. 6A and Fig. 6B, respectively) and uniform contraction (Video S7 and Video S8, respectively), confirming the robustness of our method. Moreover, to characterize the mechanical function of the spontaneously beating human cardiac grafts, we determined the contractile strain of hPSCs-CLCs seeded on vdECM by measuring the relative cardiac graft deformation in the direction of maximal tissue contraction. Human cardiac grafts exhibited a 3.78-fold increase in strain compared to hPSCs-CLCs cultured on matrigel (15.53 ± 3.33% and 4.21± 0.93%, respectively) (Fig. S14; Video S9 and Video S10). These results are in agreement with previous findings when analyzing myocardial strain in the human heart [40].

Supplementary video related to this article can be found at http://dx.doi.org/10.1016/j.biomaterials.2016.04.003.

3.4. Human vdECMs promote a higher degree of differentiation in hPSCs-CLCs when compared to matrigel, as assessed by electrophysiological and molecular analysis

Next, we sought to evaluate if hPSCs-CLCs grown either on vdECMs or matrigel presented electrically and mechanically connected functional activity. Simultaneous recording of voltage and calcium demonstrated the coordinated activity of cardiac structures for all cases, indicating the functional gap junctions' interconnection between hPSCs-CLCs (Fig. 7A, B). Maturation degree was evaluated by comparing the main electrophysiological properties from optical mapping recordings at 1 Hz pacing rate [(i.e. wavefront propagation conduction velocity (CV), mean action potential duration at 90% repolarization (APD90), mean calcium transient duration at 90% return to baseline (CaT90), and Ca2+ (Ca) Upstroke Time] (Fig. 7C–F). We observed a dramatic increase in the CV when

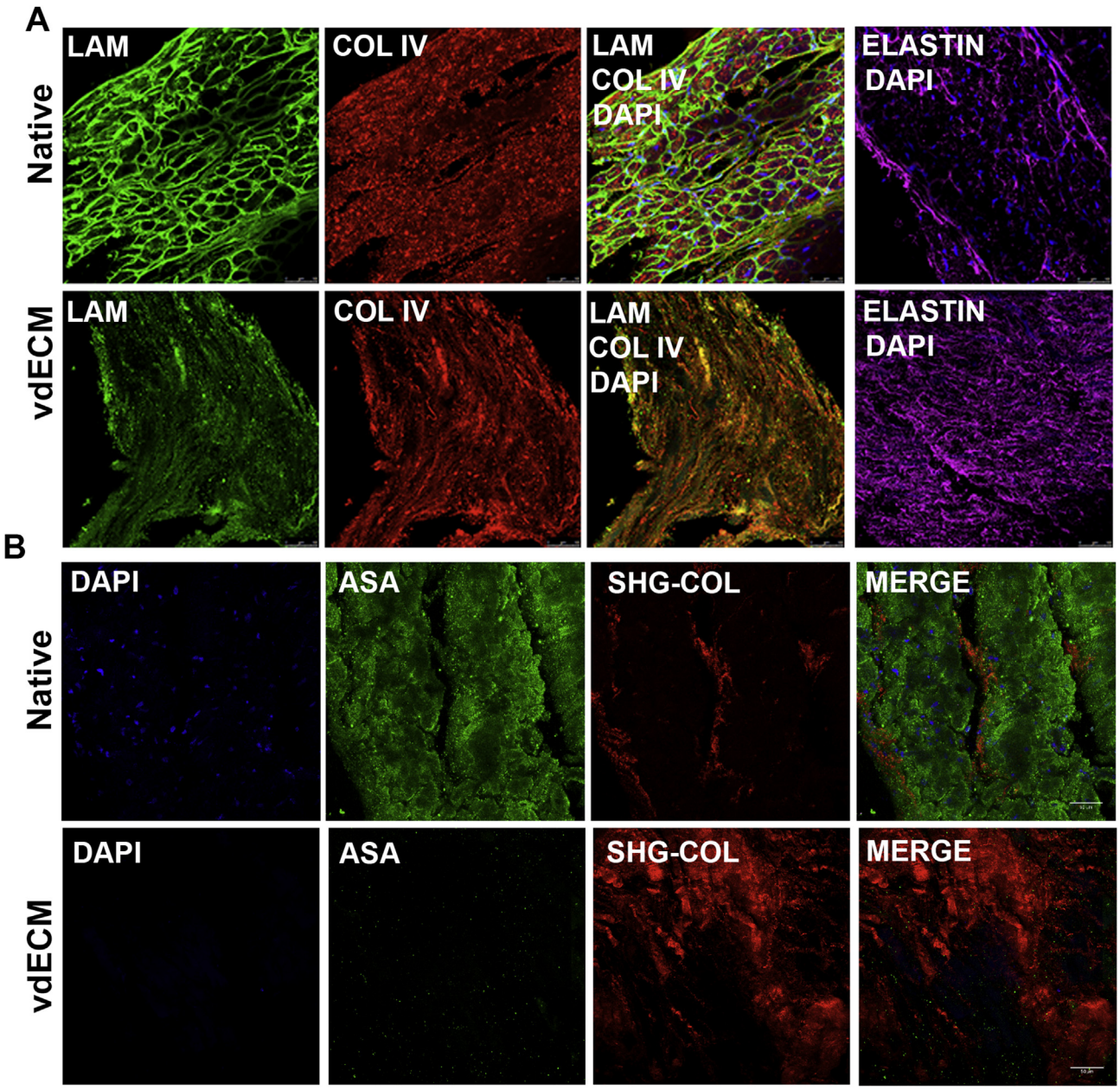

Fig. 4. Characterization of vdECMs composition. **A** Immunofluorescence analysis for LAMININ (LAM), COLLAGEN IV (COL IV), ELASTIN (ELASTIN) and DAPI staining in native human heart (Native) and vdECMs (scale bars, 50 μm). **B** Native human heart and vdECMs were analyzed by Second harmonic generation (SHG) for the detection of Collagen (SHG-Col) and by immunofluorescence analysis for ASA and DAPI staining (scale bars, 50 μm).

hESC-CLCs were cultured on top of vdECMs compared to matrigel (7.45 ± 0.94 cm/s versus 2.54 ± 0.75 cm/s) (Fig. 7C). Similar results were observed for FiPS#1-CLCs (8.30 ± 0.49 cm/s versus 2.03 ± 0.18 cm/s, respectively) (Fig. 7C). Increases in CV when hPSCs-CLCs were cultured on vdECMs were related to a higher degree of excitability of sodium current, as 10 μM flecaidine infusion resulted in a more significant reduction of the conduction velocity of hPSCs-CLCs (i.e. 63 ± 9% versus 44 ± 11% for hESC-CLCs and 71 ± 13% versus 41 ± 5% for FiPS#1-CLCs) (Fig. 7H).

To assess if increases in the CV were also associated with higher contraction capability due to differences in culture substrates, we evaluated the kinetics of calcium as an indicative parameter of hPSCs-CLCs maturation. hPSCs-CLCs cultured on vdECMs showed a reduction in the duration of CaT90 and calcium upstroke time compared to matrigel (Fig. 7E, F). Such variations were not associated with significant differences in the duration of APD90 (Fig. 7D). Specifically, faster calcium transient increases in hESC-CLCs cultured on vdECMs were associated with a higher degree of maturation of late inward calcium current (I_{CaL}), since 4 μM verapamil infusion resulted in a more significant reduction of the upstroke velocity of the calcium transient (Fig. 7G).

Moreover, we investigated if such findings could correlate with differences at the level of mRNA expression (Fig. 7I). Increases in the levels of expression of SCN5A mRNA when hPSCs-CLCs were cultured on vdECMs compared to matrigel condition were in agreement with increases in conduction velocities (Fig. 7C, H). Similar results were found for inward rectifier potassium current (KCNJ2). Interestingly, increases in KCNJ2 are associated with lower resting potential in cardiomyocytes, leading to higher conduction velocities [41], as observed in Fig. 7C. So far, acquisition of KCNJ2

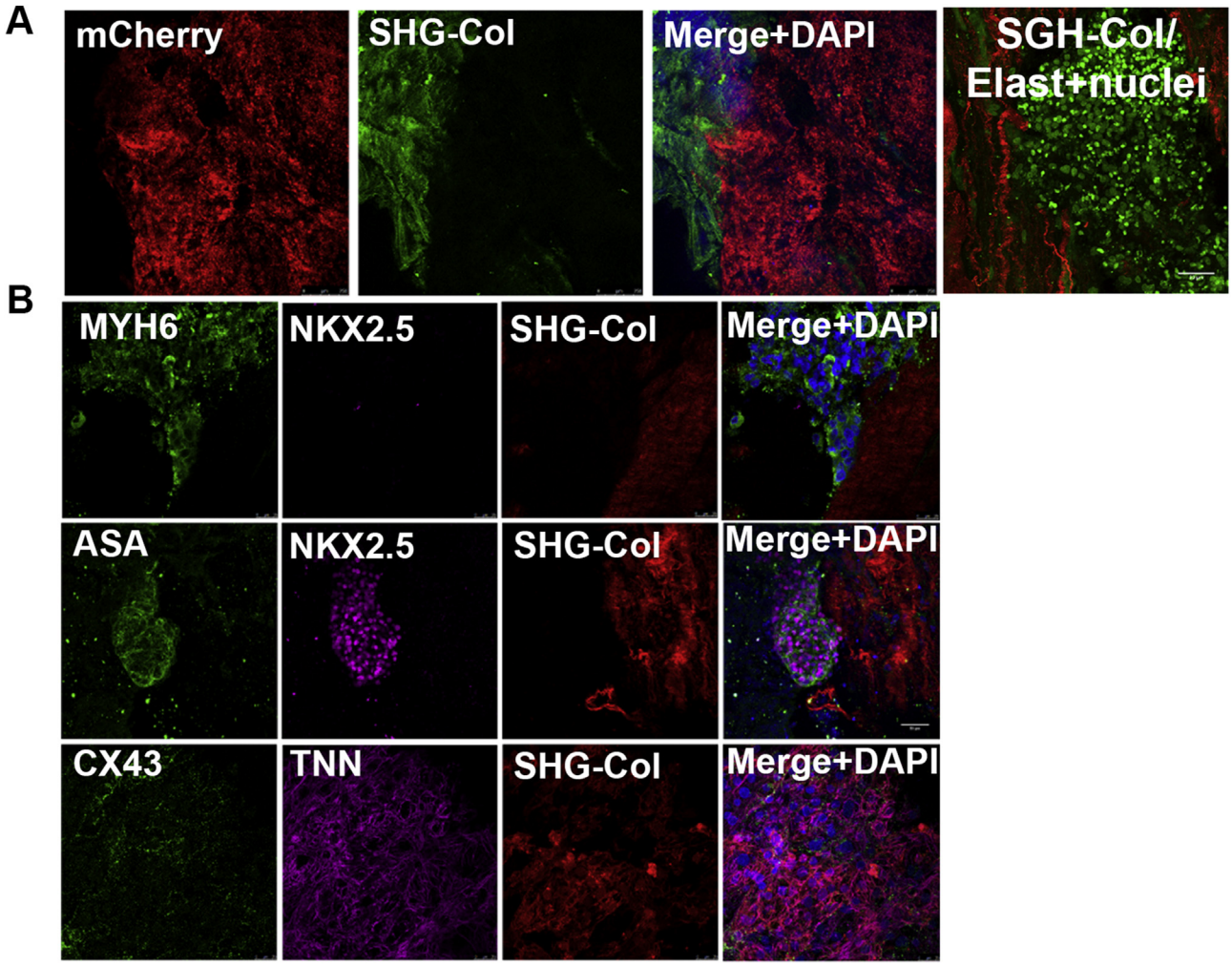

Fig. 5. Cardiac differentiation of ES4 mCherry_MHY6 derived CLCs on vdECMs. A *Left panels*, ES4 mCherry_MHY6 derived CLCs were cultured on top of vdECMs during 10 days and further analyzed for mCherry fluorescence together with the detection of collagen from the underlying vdECM by Second Harmonic Generation (SHG-Col) (scale bars, 250 μm). *Right panel*, higher magnification image showing the fibrillary microstructure of collagen from the underlying vdECM and elastin/nuclei by SHG-TPEF (scale bar, 50 μm). **B** Immunofluorescence analysis for: *Top panels*, MYH6, Nkx2.5 and detection of collagen by SHG (SHG-Col), (scale bars 25 μm). *Middle panels*, ASA, NKX2.5 and SHG-Col (scale bars 50 μm). *Bottom panels*, CX43, TNN and SHG-Col (scale bars 25 μm).

mRNA expression has been predicted as a limiting step for CLCs production from hPSCs [41], indicating that under our defined conditions, vdECMs may play a role in the expression of this current. Similarly, increases in the levels of expression of KCNA4 mRNA in hPSCs-CLCs suggested that vdECM, rather than matrigel, may represent a more physiological microenvironment for the proper differentiation of hPSCs-CLCs.

In order to ascertain the effect of the different substrates on intracellular calcium homeostasis, mRNA expression levels of the CACNA1C subunit from the L-type calcium channel current, and sarco/endoplasmic reticulum Ca2+ ATPase (SERCA) pump were investigated. Interestingly, hPSCs-CLCS co-cultured on vdEMCs compared to matrigel, exhibited higher levels of expression of CACNA1C and SERCA mRNAs [42], which correlated with increases in calcium upstroke (Fig. 7F, G). mRNA levels of the KCNH2 unit of the rapidly (I_{Kr}) activating delayed rectifier potassium channel and KCNQ1/2 [(two members of the potassium voltage-gated channel subfamily Q of the slowly (I_{Ks}) activating delayed rectifier potassium channels)] were differentially regulated when hPSCs-CLCs were cultured on matrigel or vdECMs conditions. These findings may explain the similar duration of action potentials observed (Fig. 7D). Altogether, our results suggest a pivotal role of vdECMs in providing a suitable microenvironment for the *in vitro* generation of hPSC-derived cardiac grafts.

4. Discussion

In humans, the existence of scar tissue following myocardial infarction indicates that the ability to generate new cardiomyocytes after pathological conditions is completely absent. Given that heart disease is the most significant cause of morbidity and mortality worldwide, the possibility to replace fibroblastic-like scar has been one the major goals in the cardiac field in the last years. So far, different cell therapy approaches have been proposed: from the use of allogenic cell sources alone or in combination with biomimetic materials to the possibility to reprogram *in situ* cardiac fibroblasts. In an attempt to provide novel platforms for heart regeneration, heart engineering has been envisioned as a promising approach for the generation of donor grafts. Recently, the generation of acellular matrices from different organs by decellularization has emerged as an encouraging technology to produce tissue scaffolds that retain the main properties of the organ ECM [7,8]. Within the last years, different groups, including us, have faced major problems when developing efficient protocols for heart decellularization. In this

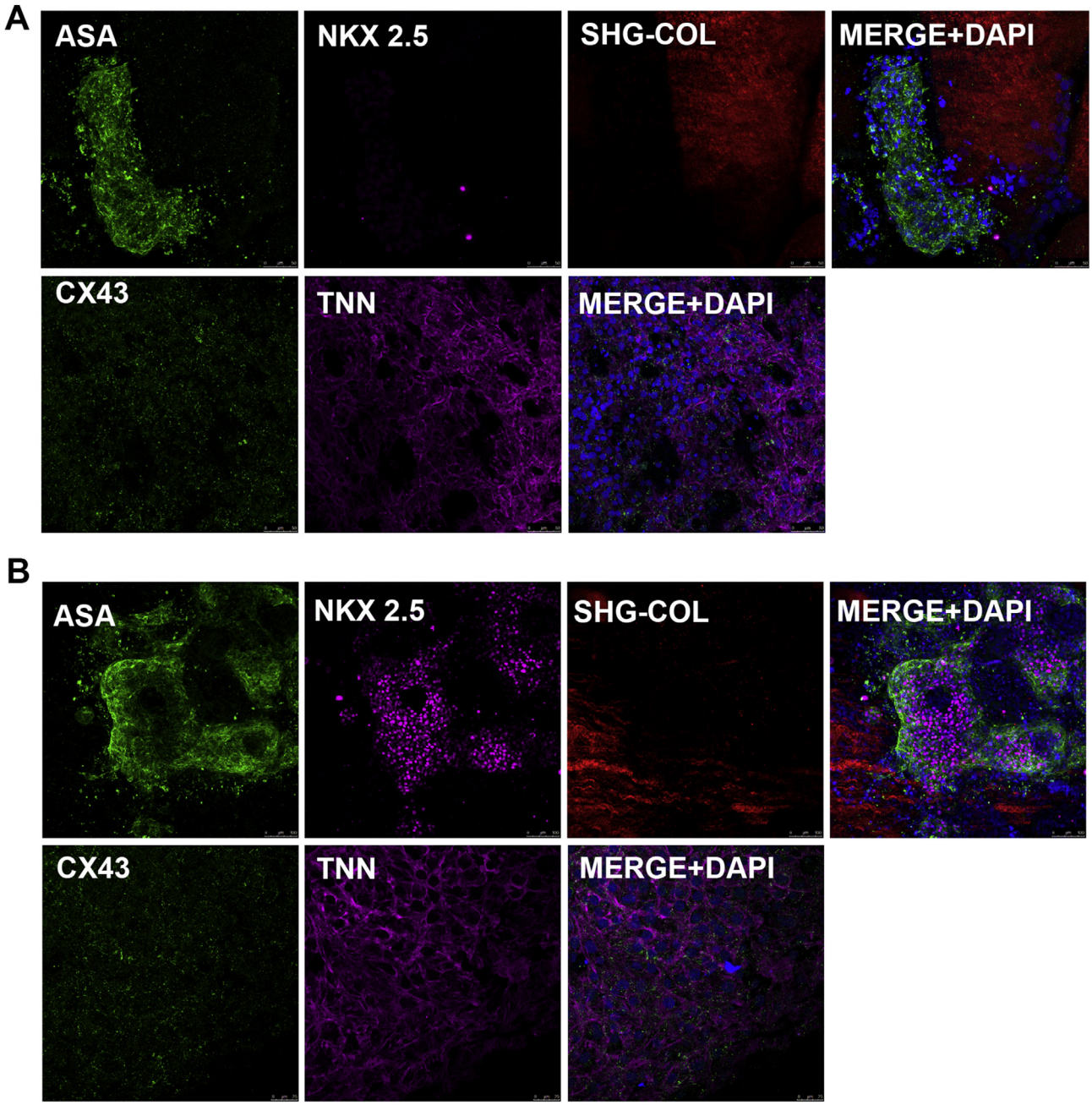

Fig. 6. Cardiac differentiation of hESC- and hiPSC- CLCs on vdECMs. A ES4-CLCs and **B** FiPS#1-CLCs were seeded on top of vdECMs during 10 days and further analyzed by immunofluorescence analysis for ASA and NKX2.5 (*top panels* in A and B), and CX43 and TNN (*bottom panels* in A and B) together with the detection of collagen by SHG (SHG-Col). Scale bars in A, 50 μm. Scale bars in B, 100 μm (*top panels*) and 25 μm (*bottom panels*).

regard, we have recently described that is possible to apply perfusion decellularization in human hearts, leading to a structurally intact decellularized extracellular matrix (dECM) preserving ultra- and macro-structures together with mechanical properties [5].

Besides the definition of suitable strategies for organ engineering, the choice of cell type for cardiac recellularization limits further applications in clinics. Lately hPSCs, such as hESCs and hiPSCs, have been heralded as major cell sources for regenerative applications, including heart engineering. hPSCs exhibit the capability to differentiate under the appropriated stimuli to cells from the three germ layers of the embryo, both *in vitro* and *in vivo*. These capabilities offer great advantages when trying to develop autologous cells for transplantation. However, protocols for cardiac differentiation of hPSCs are frequently based on the formation of EBs, hampering the reproducibility and scale up of such procedures in clinics [3,12,13]. Lately, we have demonstrated that is possible to induce cardiac differentiation from hPSCs grown as monolayers, making use of chemically defined media [16]. Although valuable, those protocols still cannot provide definitive information on the identity of the generated cells [14,16]. In this regard, the generation of cardiac hPSCs reporter cell lines can help to the identification and purification of different cardiac cell types during the onset of differentiation (i.e: cardiac mesoderm precursors, cardiac progenitor cells, mature cardiomyocytes, among others), and importantly, to develop efficient and robust protocols to generate the required

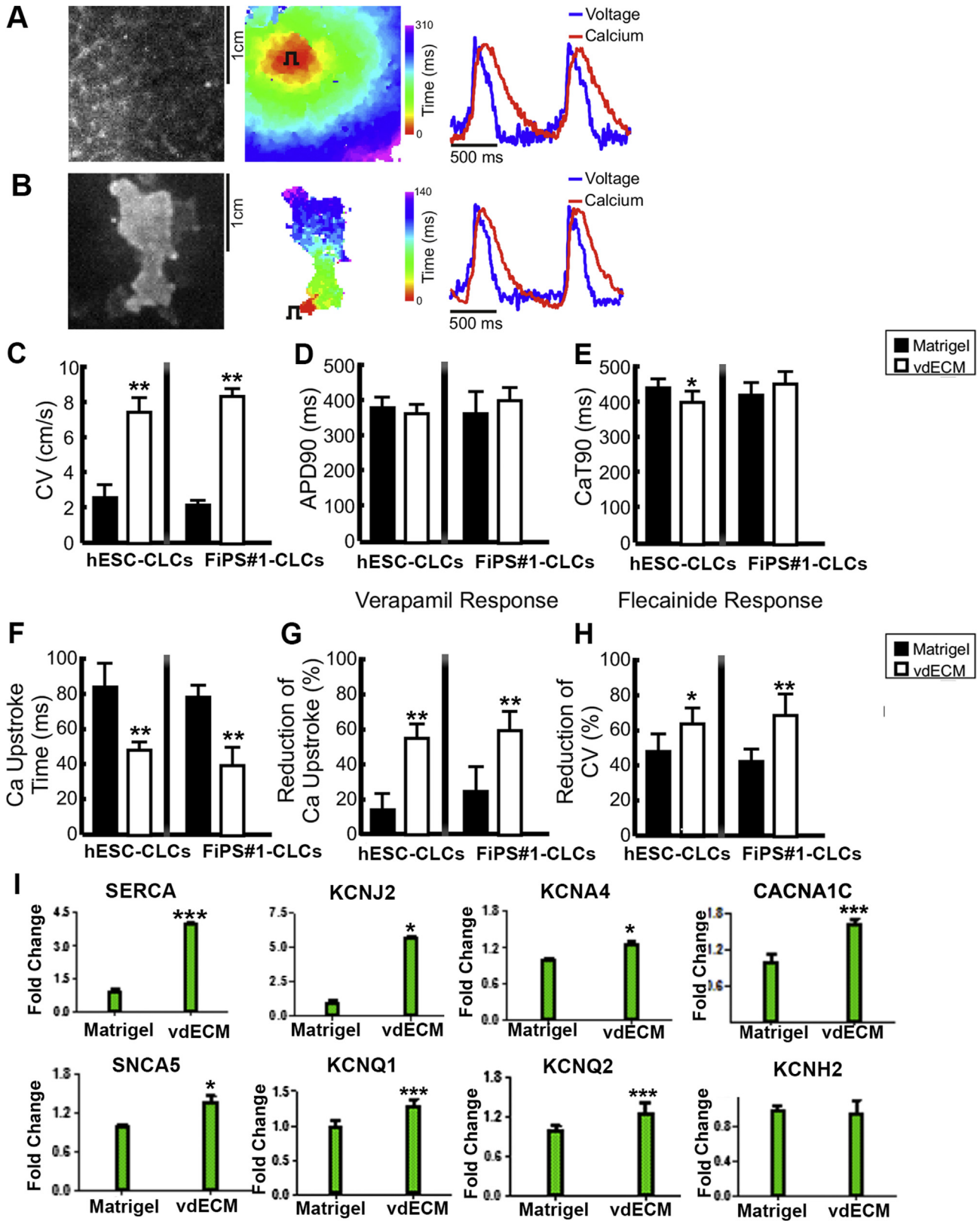

Fig. 7. Simultaneous optical mapping of transmembrane voltage and intracellular transient calcium of cardiac structures from hPSCs grown on vdECMs and matrigel. A, B Simultaneous optical mapping of transmembrane voltage and intracellular transient calcium of hPSCs-CLCs on matrigel (**A**) and vdECMs (**B**). Grayscale images of normalized fluorescence intensity map. Middle panel illustrate the propagation of transmembrane voltage. Right panels represent transmembrane voltage (blue) and calcium transient (red) traces of representative recorded pixels. **C**–**F**. Electrophysiological properties of hECS-CLCs and FiPS#1-CLCs grown on matrigel and vdECMs: **C** wavefront propagation conduction velocity, **D** action potential duration (APD90), **E** calcium transient duration (CaT90) and **F** Calcium (Ca) upstroke time measured on hECS-CLCs and FiPS#1-CLCs grown on matrigel and vdECMs. **G** Effect of verapamil on reduction of Ca upstroke time. **H** Effect of flecainide on reduction of conduction velocity. **I** mRNA analysis by qPCR for the indicated markers ($n = 3$) (*$p < 0.05$; **$p < 0.01$, ***$p < 0.001$).

amount of cardiac cells needed in the clinical setting.

Recent genome editing technologies including CRISPR/Cas9 and TALEN platforms have demonstrated to target unique and multiple human loci in site-specific manner. Interestingly, recent works have investigated the impact of genome editing platforms in the incidence of off-target mutations. In this regard it has been shown that off-target mutations attributable to the nucleases were rarely exhibited in CRISPR-Cas9 and TALEN targeted hPSCs clones [43]. We have also recently interrogated by whole-genome sequencing the mutational load in individual gene-corrected hiPSC clones at single-base resolution, showing that gene correction by helper-dependent adenoviral vector (HDAdV) or TALEN exhibited few off-target effects and a low level of sequence variation [44]. Importantly, others have described the generation of a high-fidelity Cas9 variant (named SpCas9-HF1) designed to reduce non-specific DNA interactions, showing no detectable genome-wide off-target effects [45].

Here we decided to take advantage of TALEN platform to target MYH6 locus with mCherry fluorescent reporter in order to generate a reporter cell line mirroring MYH6 endogenous activity during the onset of cardiac differentiation. In the present work, we have derived three different mCherry MYH6 reporter hESC lines that serve as an unprecedented scenario for the definition of a chemically defined protocol for cardiac differentiation of hPSCs. In our hands, gene targeting and subsequent cell culture pressure did not hamper ES4 mCherry_MYH6 line to exhibit typical pluripotent-related features, as described by others when targeting other human locus by means of this approach [24,29,46–48]. Following our cardiac differentiation protocol, CLCs expressing mCherry fluorescent protein were generated in only 7 days, mirroring MYH6 endogenous expression. Moreover, we could successfully apply the same cardiac differentiation strategy to hPSCs lines, demonstrating the suitability of our protocol for the generation of CLCs from monolayer cultures of different hPSCs lines. In our hands, TALEN engineering allowed not only to generate for the first time a hESCs cardiac reporter cell line by means of this genome editing platform, but also, to define a robust protocol of cardiac differentiation from hPSCs.

Important cell functions such as proliferation and differentiation can be modulated by the biochemical and biophysical properties of their microenvironment [49–51]. Mechanical cues from the ECM including rigidity, microstructure and 3D architecture have shown to exert changes in intracellular cell signaling cascades and subsequently drive cell fate [52–54]. Elegant studies have previously shown the benefits when using murine cardiac ECM in promoting cardiac differentiation from hPSCs [9,11]. Also, others have recently demonstrated that engineered heart slices from pig and rat represented a suitable platform for the culture of neonatal rat ventricular cardiomyocytes, behaving as an integrated and functional tissue-like constructs [10]. Understanding cellular interactions of CLCs with the ECM of human origin can have important implications in the development of functional tissue engineered grafts from hPSCs. Here, we show that hPSCs-CLCs co-cultured on human vdECMs for 10 days displayed better electrophysiological responses compared to matrigel, which is mostly used to produce high yields of cardiomyocytes from hPSCs. Importantly, our findings were together in agreement with increases in the expression of different cardiac channels such as SNCA5, KCNJ2, KCNA4, CACNA1C, SERCA2, KCNQ1, and KCNQ2, pinpointing a pivotal role of human cardiac ECM as an inducer of cardiac-related electrophysiological features.

5. Conclusions

Decellularization of a whole heart can lead to hundreds of acellular slices ready to use as scaffolds for the approach described here. The present protocol allows for the generation of cardiac grafts showing enhanced electrophysiological properties in a relatively short time period (24 days), avoiding time consuming co-culture techniques (i.e: bioreactor, perfusion system, among others), and anticipating that such procedure can be immediately applied in laboratories with special focus in heart bioengineering and cardiac disease modeling.

Disclosures

None.

Sources of funding

E.G was partially supported by La Fundació Privada La Marató de TV3, 121430/31/32 and Spanish Ministry of Economy and Competitiveness-MINECO (SAF2014-59778). L.O was supported by grants from Spanish Ministry of Economy and Competitiveness-MINECO (BFU2009-13513 and SAF2014-59778) and by La Fundació Privada La Marató de TV3 (121430/31/32). M.E.F, A.C and F.F.A from Instituto de Salud Carlos III-ISCII (MINECO: PI10-00141 and PI10-02038), Red de Investigación Cardiovascular (RIC) and Red TerCel from ISCII (Ministry of Economy and Competitiveness, Spain) and CAM: S2010/BMD-2420. R.O was founded by Secretaria d'Universitats i Recerca del Departament d'Economia i Coneixement de la Generalitat de Catalunya. E.M and M.V by 2014 SGR 1442. J.C.I.B. was supported by grants from the G. Harold and Leila Y. Mathers Charitable Foundation, The Leona M. and Harry B. Helmsley Charitable Trust (2012-PG-MED002) and The Moxie Foundation. N.M was partially supported by StG-2014-640525_REGMAMKID, La Fundació Privada La Marató de TV3 (121430/31/32), MINECO (SAF2014-59778 and BFU2009-13513), the Spanish Ministry of Science and Innovation (PLE 2009-147) and 2014 SGR 1442.

Acknowledgments

Authors gratefully acknowledge the help of M. Schwarz, P. Schwarz, and Ana Fernández Baza for administrative help and logistic coordination. TALEN Backbone was a gift from Feng Zhang. We also thank all the medical, nursing staff, and personnel in the Hospital General Universitario Gregorio Marañón, the University of Minnesota, the Texas Heart Institute, and the ONT who made the study possible. Most of all, we thank all the relatives of each donor patient for donating specifically the hearts to be used for this investigational purpose; without their help and support science would never advance.

Appendix A. Supplementary data

Supplementary data related to this article can be found at http://dx.doi.org/10.1016/j.biomaterials.2016.04.003.

References

[1] J.A. Thomson, Embryonic stem cell lines derived from human blastocysts, Sci. (80-) 282 (1998) 1145–1147, http://dx.doi.org/10.1126/science.282.5391.1145.

[2] K. Takahashi, K. Tanabe, M. Ohnuki, M. Narita, T. Ichisaka, K. Tomoda, et al., Induction of pluripotent stem cells from adult human fibroblasts by defined factors, Cell 131 (2007) 861–872, http://dx.doi.org/10.1016/j.cell.2007.11.019.

[3] C.L. Mummery, J. Zhang, E.S. Ng, D.A. Elliott, A.G. Elefanty, T.J. Kamp, Differentiation of human embryonic stem cells and induced pluripotent stem cells to cardiomyocytes: a methods overview, Circ. Res. 111 (2012) 344–358, http://dx.doi.org/10.1161/CIRCRESAHA.110.227512.

[4] J.P. Guyette, J. Charest, R.W. Mills, B. Jank, P.T. Moser, S.E. Gilpin, J.R. Gershlak, T. Okando, T. Okamoto, G. Gonzalez, D.J. Milan, G.R. Gaudette, H.C. Ott, Bioengineering human myocardium on native extracellular matrix, Circ. Res. 118 (2016) 56–72.

[5] P.L. Sánchez, M.E. Fernández-Santos, S. Costanza, A.M. Climent, I. Moscoso, M.A. Gonzalez-Nicolas, et al., Acellular human heart matrix: a critical step toward whole heart grafts, Biomaterials 61 (2015) 279–289, http://dx.doi.org/10.1016/j.biomaterials.2015.04.056.

[6] H.C. Ott, T.S. Matthiesen, S.-K. Goh, L.D. Black, S.M. Kren, T.I. Netoff, et al., Perfusion-decellularized matrix: using nature's platform to engineer a bioartificial heart, Nat. Med. 14 (2008) 213–221, http://dx.doi.org/10.1038/nm1684.

[7] D. Rana, H. Zreiqat, N. Benkirane-Jessel, S. Ramakrishna, M. Ramalingam, Development of decellularized scaffolds for stem cell-driven tissue engineering, J. Tissue Eng. Regen. Med. (2015), http://dx.doi.org/10.1002/term.2061.

[8] L.F. Tapias, H.C. Ott, Decellularized scaffolds as a platform for bioengineered organs, Curr. Opin. Organ Transpl. 19 (2014) 145–152, http://dx.doi.org/10.1097/MOT.0000000000000051.

[9] S.L.J. Ng, K. Narayanan, S. Gao, A.C.A. Wan, Lineage restricted progenitors for the repopulation of decellularized heart, Biomaterials 32 (2011) 7571–7580, http://dx.doi.org/10.1016/j.biomaterials.2011.06.065.

[10] A. Blazeski, G.M. Kostecki, L. Tung, Engineered heart slices for electrophysiological and contractile studies, Biomaterials 55 (2015) 119–128, http://dx.doi.org/10.1016/j.biomaterials.2015.03.026.

[11] T.Y. Lu, B. Lin, J. Kim, M. Sullivan, K. Tobita, G. Salama, et al., Repopulation of decellularized mouse heart with human induced pluripotent stem cell-derived cardiovascular progenitor cells, Nat. Commun. 4 (2013) 2307, http://dx.doi.org/10.1038/ncomms3307.

[12] N. Cao, Z. Liu, Z. Chen, J. Wang, T. Chen, X. Zhao, Y. Ma, L. Qin, J. Kang, B. Wei, L. Wang, Y. Jin, H.T. Yang, Ascorbic acid enhances the cardiac differentiation of induced pluripotent stem cells through promoting the proliferation of cardiac progenitor cells, Cell Res. 22 (2011) 219–236.

[13] R.P. Davis, S. Casini, C.W. Van Den Berg, M. Hoekstra, C.A. Remme, C. Dambrot, et al., Cardiomyocytes derived from pluripotent stem cells recapitulate electrophysiological characteristics of an overlap syndrome of cardiac sodium channel disease, Circulation 125 (2012) 3079–3091, http://dx.doi.org/10.1161/CIRCULATIONAHA.111.066092.

[14] X. Lian, C. Hsiao, G. Wilson, K. Zhu, L.B. Hazeltine, S.M. Azarin, et al., Robust cardiomyocyte differentiation from human pluripotent stem cells via temporal modulation of canonical Wnt signaling, Proc. Natl. Acad. Sci. U. S. A. 109 (2012) E1848–E1857, http://dx.doi.org/10.1073/pnas.1200250109.

[15] X. Lian, J. Zhang, S.M. Azarin, K. Zhu, L.B. Hazeltine, X. Bao, et al., Directed cardiomyocyte differentiation from human pluripotent stem cells by modulating Wnt/β-catenin signaling under fully defined conditions, Nat. Protoc. 8 (2013) 162–175, http://dx.doi.org/10.1038/nprot.2012.150.

[16] Y. Gu, G.-H. Liu, N. Plongthongkum, C. Benner, F. Yi, J. Qu, et al., Global DNA methylation and transcriptional analyses of human ESC-derived cardiomyocytes, Protein Cell 5 (2014) 59–68, http://dx.doi.org/10.1007/s13238-013-0016-x.

[17] J. Zhang, M. Klos, G.F. Wilson, A.M. Herman, X. Lian, K.K. Raval, et al., Extracellular matrix promotes highly efficient cardiac differentiation of human pluripotent stem cells: the matrix sandwich method, Circ. Res. 111 (2012) 1125–1136, http://dx.doi.org/10.1161/CIRCRESAHA.112.273144.

[18] D.A. Elliott, S.R. Braam, K. Koutsis, E.S. Ng, R. Jenny, E.L. Lagerqvist, et al., NKX2-5eGFP/w hESCs for isolation of human cardiac progenitors and cardiomyocytes, Nat. Methods 8 (2011) 1037–1040, http://dx.doi.org/10.1038/nmeth.1740.

[19] S.C. Den Hartogh, C. Schreurs, J.J. Monshouwer-Kloots, R.P. Davis, D.A. Elliott, C.L. Mummery, et al., Dual reporter MESP1 mCherry/w -NKX2-5 eGFP/w hESCs enable studying early human cardiac differentiation, Stem Cells 33 (2015) 56–67, http://dx.doi.org/10.1002/stem.1842.

[20] T.I. Orbán, A. Apáti, A. Németh, N. Varga, V. Krizsik, A. Schamberger, K. Szébenyi, Z. Erdei, G. Várady, E. Karászi, L. Homolya, K. Német, E. Gócza, C. Miskey, L. Mátés, Z. Ivics, Z. Izsvák, B. Sarkadi, Applying a "double-feature" promoter to identify cardiomyocytes differentiated from human embryonic stem cells following transposon-based gene delivery, Stem Cells 27 (2009) 1077–1087.

[21] K. Szebenyi, A. Pentek, Z. Erdei, G. Varady, T.I. Orban, B. Sarkadi, et al., Efficient generation of human embryonic stem cell-derived cardiac progenitors based on tissue-specific enhanced green fluorescence protein expression, Tissue Eng. Part C Methods 21 (2015) 35–45, http://dx.doi.org/10.1089/ten.TEC.2013.0646.

[22] M. Ieda, J.D. Fu, P. Delgado-Olguin, V. Vedantham, Y. Hayashi, B.G. Bruneau, et al., Direct reprogramming of fibroblasts into functional cardiomyocytes by defined factors, Cell 142 (2010) 375–386, http://dx.doi.org/10.1016/j.cell.2010.07.002.

[23] T.W. Gilbert, J.M. Freund, S.F. Badylak, Quantification of DNA in biologic scaffold materials, J. Surg. Res. 152 (2009) 135–139, http://dx.doi.org/10.1016/j.jss.2008.02.013.

[24] N.E. Sanjana, L. Cong, Y. Zhou, M.M. Cunniff, G. Feng, F. Zhang, A transcription activator-like effector toolbox for genome engineering, Nat. Protoc. 7 (2012) 171–192, http://dx.doi.org/10.1038/nprot.2011.431.

[25] J.C. Miller, S. Tan, G. Qiao, K.A. Barlow, J. Wang, D.F. Xia, et al., A TALE nuclease architecture for efficient genome editing, Nat. Biotechnol. 29 (2011) 143–148, http://dx.doi.org/10.1038/nbt.1755.

[26] C. Engler, R. Gruetzner, R. Kandzia, S. Marillonnet, Golden gate shuffling: a one-pot DNA shuffling method based on type IIs restriction enzymes, PLoS One 4 (2009) e5553, http://dx.doi.org/10.1371/journal.pone.0005553.

[27] E. Weber, C. Engler, R. Gruetzner, S. Werner, S. Marillonnet, A modular cloning system for standardized assembly of multigene constructs, PLoS One 6 (2011) 38–43, http://dx.doi.org/10.4161/bbug.3.1.18223.

[28] E.L. Doyle, N.J. Booher, D.S. Standage, D.F. Voytas, V.P. Brendel, J.K. Vandyk, et al., TAL Effector-Nucleotide Targeter (TALE-NT) 2.0: tools for TAL effector design and target prediction, Nucleic Acids Res. 40 (2012) 117–122, http://dx.doi.org/10.1093/nar/gks608.

[29] D. Hockemeyer, H. Wang, S. Kiani, C.S. Lai, Q. Gao, P. John, et al., Genetic engineering of human ES and iPS cells using TALE nucleases, Nat. Biotechnol. 29 (2012) 731–734, http://dx.doi.org/10.1038/nbt.1927.Genetic.

[30] J. Courchet, T.L. Lewis, S. Lee, V. Courchet, D.Y. Liou, S. Aizawa, et al., XTerminal axon branching is regulated by the LKB1-NUAK1 kinase pathway via presynaptic mitochondrial capture, Cell 153 (2013) 1510–1525, http://dx.doi.org/10.1016/j.cell.2013.05.021.

[31] G.-H. Liu, K. Suzuki, M. Li, J. Qu, N. Montserrat, C. Tarantino, et al., Modelling Fanconi anemia pathogenesis and therapeutics using integration-free patient-derived iPSCs, Nat. Commun. 5 (2014) 4330, http://dx.doi.org/10.1038/ncomms5330.

[32] K. Okita, Y. Matsumura, Y. Sato, A. Okada, A. Morizane, S. Okamoto, et al., A more efficient method to generate integration-free human iPS cells, Nat. Methods 8 (2011) 409–412, http://dx.doi.org/10.1038/nmeth.1591.

[33] T. Aasen, A. Raya, M.J. Barrero, E. Garreta, A. Consiglio, F. Gonzalez, et al., Efficient and rapid generation of induced pluripotent stem cells from human keratinocytes, Nat. Biotechnol. 26 (2008) 1276–1284, http://dx.doi.org/10.1038/nbt.1503.

[34] M.A. Wallenburg, J. Wu, R.-K. Li, I.A. Vitkin, Two-photon microscopy of healthy, infarcted and stem-cell treated regenerating heart, J. Biophot. 4 (2011) 297–304, http://dx.doi.org/10.1002/jbio.201000059.

[35] N. Merna, C. Robertson, A. La, S.C. George, Optical imaging predicts mechanical properties during decellularization of cardiac tissue, Tissue Eng. Part C. Methods 19 (2013) 802–809, http://dx.doi.org/10.1089/ten.TEC.2012.0720.

[36] E. Melo, E. Garreta, T. Luque, J. Cortiella, J. Nichols, D. Navajas, et al., Effects of the decellularization method on the local stiffness of acellular lungs, Tissue Eng. Part C. Methods 20 (2014) 412–422, http://dx.doi.org/10.1089/ten.TEC.2013.0325.

[37] P. Lee, M. Klos, C. Bollensdorff, L. Hou, P. Ewart, T.J. Kamp, et al., Simultaneous voltage and calcium mapping of genetically purified human induced pluripotent stem cell-derived cardiac myocyte monolayers, Circ. Res. 110 (2012) 1556–1563, http://dx.doi.org/10.1161/CIRCRESAHA.111.262535.

[38] P. Lee, F. Taghavi, P. Yan, P. Ewart, E.A. Ashley, L.M. Loew, et al., In situ optical mapping of voltage and calcium in the heart, PLoS One 7 (2012) e42562, http://dx.doi.org/10.1371/journal.pone.0042562.

[39] P.M. Crapo, T.W. Gilbert, S.F. Badylak, An overview of tissue and whole organ decellularization processes, Biomaterials 32 (2011) 3233–3243, http://dx.doi.org/10.1016/j.biomaterials.2011.01.057.

[40] J. Garot, D.A. Bluemke, N.F. Osman, C.E. Rochitte, E.R. McVeigh, E.A. Zerhouni, et al., Fast determination of regional myocardial strain fields from tagged cardiac images using harmonic phase MRI, Circulation 101 (2000) 981–988, http://dx.doi.org/10.1161/01.CIR.101.9.981.

[41] M. Hoekstra, C.L. Mummery, A.A.M. Wilde, C.R. Bezzina, A.O. Verkerk, Induced pluripotent stem cell derived cardiomyocytes as models for cardiac arrhythmias, Front. Physiol. 3 AUG (2012) 1–14, http://dx.doi.org/10.3389/fphys.2012.00346.

[42] D.M. Bers, Calcium fluxes involved in control of cardiac myocyte contraction, Circ. Res. 87 (2000) 275–281.

[43] A. Veres, B.S. Gosis, Q. Ding, R. Collins, A. Ragavendran, H. Brand, S. Erdin, A. Cowan, M.E. Talkowski, K. Musunuru, Low incidence of off-target mutations in individual CRISPR-Cas9 and TALEN targeted human stem cell clones detected by whole-genome sequencing, Cell Stem Cell 15 (2014) 27–30.

[44] K. Suzuki, C. Yu, J. Qu, M. Li, X. Yao, T. Yuan, et al., Targeted gene correction minimally impacts whole-genome mutational load in human-disease-specific induced pluripotent stem cell clones, Cell Stem Cell 15 (2014) 31–36, http://dx.doi.org/10.1016/j.stem.2014.06.016.

[45] B.P. Kleinstiver, V. Pattanayak, M.S. Prew, S.Q. Tsai, N.T. Nguyen, Z. Zheng, et al., High-fidelity CRISPR–Cas9 nucleases with no detectable genome-wide off-target effects, Nature (2016), http://dx.doi.org/10.1038/nature16526.

[46] N.A. Krentz, C. Nian, F. Lynn, TALEN/CRISPR-mediated eGFP knock-in add-on at the OCT4 locus does not impact differentiation of human embryonic stem cells towards endoderm, PLoS One 9 (2014) e114275.

[47] H. Pan, W. Zhang, W. Zhang, G.-H. Liu, Find and replace: editing human genome in pluripotent stem cells, Protein Cell 2 (2011) 950–956, http://dx.doi.org/10.1007/s13238-011-1132-0.

[48] D.A. Ovchinnikov, D.M. Titmarsh, P.R.J. Fortuna, A. Hidalgo, S. Alharbi, D.J. Whitworth, et al., Transgenic human ES and iPS reporter cell lines for identification and selection of pluripotent stem cells in vitro, Stem Cell Res. 13 (2014) 251–261, http://dx.doi.org/10.1016/j.scr.2014.05.006.

[49] D.E. Discher, D.J. Mooney, P.W. Zandstra, Growth factors, matrices, and forces combine and control stem cells, Science 324 (2009) 1673–1677, http://dx.doi.org/10.1126/science.1171643.

[50] P.C.D.P. Dingal, D.E. Discher, Combining insoluble and soluble factors to steer stem cell fate, Nat. Mater 13 (2014) 532–537, http://dx.doi.org/10.1038/nmat3997.

[51] N. Huebsch, P.R. Arany, A.S. Mao, D. Shvartsman, O.A. Ali, S.A. Bencherif, et al., Harnessing traction-mediated manipulation of the cell/matrix interface to control stem-cell fate, Nat. Mater. 9 (2010) 518–526, http://dx.doi.org/

10.1038/nmat2732.
[52] J.H. Wen, L.G. Vincent, A. Fuhrmann, Y.S. Choi, K.C. Hribar, H. Taylor-Weiner, et al., Interplay of matrix stiffness and protein tethering in stem cell differentiation, Nat. Mater. Adv. (2014) 1–21, http://dx.doi.org/10.1038/nmat4051.
[53] B.M. Baker, C.S. Chen, Deconstructing the third dimension - how 3D culture microenvironments alter cellular cues, J. Cell Sci. 125 (2012) 3015–3024, http://dx.doi.org/10.1242/jcs.079509.
[54] O.F. Zouani, C. Chanseau, B. Brouillaud, R. Bareille, F. Deliane, M.-P. Foulc, et al., Altered nanofeature size dictates stem cell differentiation, J. Cell Sci. 125 (2012) 1217–1224, http://dx.doi.org/10.1242/jcs.093229.